

Electrochromic materials and devices: Brief survey and new data on optical absorption in tungsten oxide and nickel oxide films

E. Avendaño^{a,1}, L. Berggren^a, G.A. Niklasson^a, C.G. Granqvist^{a,*}, A. Azens^b

^a Department of Engineering Sciences, The Ångström Laboratory, Uppsala University, P. O. Box 534, SE-75121 Uppsala, Sweden

^b ChromoGenics Sweden AB, c/o Uppsala University Holding, Uppsala Science Park, SE-75183 Uppsala, Sweden

Available online 3 October 2005

Abstract

Current work on inorganic electrochromic materials and devices is reviewed briefly, and the emphasis on thin films of W oxide and Ni oxide is pointed out. New results are presented on the optical properties for sputter-deposited thin films of these two materials: for Li⁺ intercalated sub-stoichiometric W oxide, it is shown that the absorption can be reconciled with an extended “site saturation” model accounting for electronic transitions between W ions in 6+, 5+, and 4+ states, and for H⁺ deintercalated Ni oxide, it is found that the coloration efficiency is higher than in prior work presumably as a consequence of the nanocrystalline structure ensuing from the deposition conditions.

© 2005 Elsevier B.V. All rights reserved.

Keywords: Optoelectronic devices; Tungsten oxide; Nickel oxide; Sputtering

1. Introduction

Materials that are able to change their optical properties as a response to an external stimulus are referred to as “chromogenic” [1]. The change can be effected through irradiation by light (photochromic materials), change in temperature (thermo-chromic materials), and the application of an electrical voltage (electrochromic materials), to mention the most common alternatives. Electrochromic materials were brought to public attention some 35 years ago in seminal work on tungsten oxide films by Deb [2,3]. In essence, the optical absorption in the visible range changes between widely separated extrema as charge is inserted or extracted. These materials were immediately considered for application in information display, but they did not stand up to the competition from the then rapidly developing liquid crystal devices.

Nevertheless, electrochromism has remained an active area for basic and applied research, with large possibilities for applications in emerging technologies. The interest was boosted in the mid-1980s with the realization that electro-

chromism was of much interest in fenestration technology as a means to achieve energy efficiency in buildings [4], and the concept of the “smart window” [5]—with variable transmittance of light and solar energy—was coined and captured the interest of researchers and the general public. Since then, electrochromic materials have been considered one subset of the “solar energy materials” [6,7]. Recently, it has become clear that “smart windows” are able to combine two features that are often thought of as incompatible: energy efficiency (as a result of the curtailing of air conditioning) and indoor comfort (due to less glare and thermal discomfort [8,9]). Similar assets prevail in the automotive sector. A number of more or less related chromogenic technologies are also available [10,11], and special mention should be made of polymer-based technology for electrochromic automatically dimming rear-view mirrors [12], which are now generally available for cars and trucks. Electrochromism is possible also in a number of polymers [13].

Section 2 below introduces electrochromic device design and gives a “miniature review” of current work on electrochromic thin films. Today’s emphasis is found to be on tungsten oxide and nickel oxide. Some new results on these two materials then follow in Sections 3 and 4. Specifically, Section 3 discusses optical absorption in W oxide films with varying stoichiometry and provides evidence in favour of a “site saturation” model accounting for electron transitions

* Corresponding author. Tel.: +46 18 4713067; fax: +46 18 500131.

E-mail address: claes-goran.granqvist@angstrom.uu.se (C.G. Granqvist).

¹ Present address: LNLS, Rua Giuseppe Máximo Scolfaro 1000, Pólo II de Alta Tecnologia de Campinas, Caixa Postal 6192, Campinas, Sao Paulo, CEP 13084-971, Brazil.

between tungsten ions in different valence states, and Section 4 deals with optical absorption in Ni oxide films and shows that very large absorption can be achieved in nanocrystalline materials whose grain boundaries appear to be where the absorption takes place.

2. Survey of electrochromism

2.1. Prototype device design

Fig. 1 illustrates a standard electrochromic construction that allows basic features and operating principles to be introduced conveniently. The design embodies five superimposed layers on one substrate or positioned between two substrates in a laminate configuration. Normally, the substrates are made of glass or flexible polyester foil. The central part of the five-layer construction is a pure ion conductor (i.e., electrolyte) that can be organic (an adhesive polymer) or inorganic (often based on an oxide film). The ions should be small in order to be mobile; protons (H^+) or lithium ions (Li^+) are normally preferred. This ion conductor is in contact with an electrochromic film (W oxide being a typical example) capable of conducting electrons as well as ions. On the other side of the ion conductor is a film serving as ion storage, ideally with electrochromic properties complementary to those of the first electrochromic film (Ni oxide being a typical example).

The central three-layer structure is positioned between electrically conducting transparent films; the best material in terms of optical and electrical properties—or at least by far the most well known one—is $In_2O_3:Sn$ (referred to as Indium Tin Oxide, or ITO) [14,15], while films of $SnO_2:F$ are less costly and readily available on large area glass panes. $ZnO:Al$ is still another option. Surveys of the properties of transparent conducting oxides have been given recently [16,17]. Possibilities to replace these oxides with metal-based layers such as

$ZnS/Ag/ZnS$ [18,19] or even carbon nanotube layers [20] have been explored recently. We note in passing that In is often considered a rare and hence inherently expensive metal, but this view has been challenged in a recent study on the geology, mineralogy, and economics of indium, which states that this metal can enjoy virtually infinite growth in use without supply limitations [21].

When a voltage of the order of 1 V is applied between the transparent electrical conductors, ions will be shuttled between the ion storage film and the electrochromic film. The electrons injected from the transparent conductors then alter the optical properties. A reversal of the voltage, or short-circuiting, brings back the original properties. The coloration can be stopped at any intermediate level, and the device exhibits open-circuit memory so that the optical changes take place only when charge is moved. It is evident that the electrochromic device can be viewed as an electrical battery with its charging state manifested as optical absorption. Transfer of battery-type work to the field of electrochromics has been attempted [22,23], but much remains to be done to fully exploit the analogies of the two technologies.

2.2. Review of current work on inorganic electrochromic films

Electrochromic materials and devices have been reviewed several times in the past, and the literature up to 1993 is covered in considerable detail in books by Granqvist [24] and Monk et al. [25]. Device-related work until 2002 has been reviewed more recently [26,27]. We venture to give a snapshot of the ongoing endeavours of electrochromic oxides by listing the most recent literature, confined solely to 2004. Such work has been reported for oxides based on tungsten, iridium, vanadium, and nickel. W oxide colours under charge insertion and is referred to as a cathodic electrochromic materials, whereas oxides of Ir and Ni colour under charge

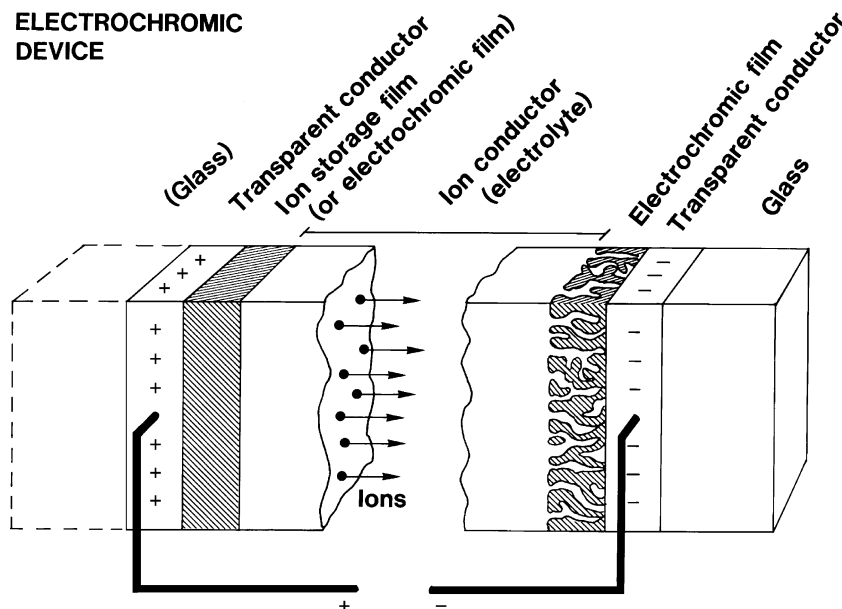


Fig. 1. Basic design of an electrochromic device, indicating transport of positive ions under the action of an electric field.

extraction and are called anodic electrochromic materials; V oxide is of an intermediate nature and displays features of weak cathodic and anodic colouration in different wavelength regions. Specifically,

- W oxide films have been prepared by evaporation [28–31], sputtering [32,33], spray pyrolysis [34], sol–gel deposition [35–40], and electrodeposition [41,42]; work has been reported also on W oxide containing Mo (made by chemical vapour deposition [43] and electrodeposition [44]), V (made by sputtering [45]), Ta (made by pulsed laser ablation [46]), Ti (made by electrodeposition [47] and spin coating followed by a templating technique [48]), and P (made by sol–gel deposition [49]);
- Ir oxide films have been prepared by electrodeposition [50,51]; work has been reported also on Ir oxide containing and Ta (made by sputtering [52]);
- V oxide films have been prepared by sputtering [53]; work has been reported also on such films with polymer additives [54]; and
- Ni oxide films have been prepared by reactive evaporation [55], pulsed laser deposition [56], sol–gel deposition [57,58], and electrodeposition [59]; work has been reported also on such sputter-deposited films containing Mg, Al, Si, V, Zr, Nb, Ag, Ta [60] as well as Au [61].

The relevant literature is much larger, though, and includes numerous investigations of similar films for sensing applications (of gases and liquids) [62], thin film batteries, super-capacitors, (electro)catalysis, etc; a survey of this work is outside the scope of the present article, though. One clear impression from this miniature review of today's literature is that the interest is focused on electrochromic W oxide and Ni oxide.

Devices incorporating electrochromic W oxide and Ni oxide films have been subject to much interest during the last decade, and detailed work has been reported on rigid (glass-based) devices [63–75] and, recently, also on flexible (polyester-film-based) devices [76,77].

3. On the electrochromism in W oxide films

3.1. Experimental

This section discusses W oxide films, with an approximate thickness of 300 nm, deposited by reactive DC magnetron sputtering in Ar+O₂ onto glass substrates coated with ITO. Detailed deposition conditions were reported in a comprehensive study by Berggren [78]. The oxygen gas flow was varied during the sputter deposition in order to accomplish large changes in the stoichiometry; the results, obtained by Elastic Recoil Detection Analysis (ERDA), were in qualitative agreement with earlier ones [79–81]. The oxygen/tungsten ratio was found to increase from 2 to 3 within a narrow range of the O₂/Ar ratio during the sputtering and then to saturate around the stoichiometric composition. The water content in the films was negligible as a consequence of the low background pressure prior to sputter deposition. The hydrogen

content was around 1 at.%, as found by ERDA. We note that over-stoichiometric films have been reported in other investigations [82]; these latter films were deposited at lower pressures and higher powers than in the present work.

The density of the W oxide films were found to be smaller the closer they were to stoichiometry. For example, WO_{2.63} had a density of ~ 7.2 g/cm³, WO_{2.89} had ~ 5.7 g/cm³, while WO_{2.93} was porous with density of ~ 5.0 g/cm³. Films with an oxygen/tungsten ratio above about 2.75 were visually transparent. For lower ratios, a progression was observed from pale purple to blue, bluish grey, brown, and finally very dark brown [78].

The as-deposited films were intercalated by Li⁺ ions in an electrolyte of lithium perchlorate in propylene carbonate. The samples were employed as working electrodes in a three-electrode electrochemical cell, and a specific amount of charge was inserted by applying a constant current over a certain time.

3.2. Optical data: Evidence for an extended site saturation model

Only W⁶⁺ is present in stoichiometric tungsten oxide, while intercalated and as-deposited films also can have W⁵⁺ states. Optical absorption can be reconciled with the site-saturation model of Denesuk and Uhlmann [83], which assumes that the optical absorption coefficient is proportional to the number of available electronic transitions from a W⁶⁺ ion to a W⁵⁺ ion. This number is found by multiplying the probabilities P for W⁶⁺ (i.e., $1-x$) and W⁵⁺ (i.e., x), where x is the Li/W ratio and is given by

$$W^{6+} \leftrightarrow W^{5+} : P = (x - x^2) \quad (1)$$

The model predicts that maximum absorption should be at $x=0.5$.

The notions underlying the site saturation model are interesting, and we now consider how they can be extended to account for optical absorption in sub-stoichiometric and Li⁺ intercalated W oxide films. Optical transmittance and reflectance were measured by spectrophotometry on sputtered deposited films having different composition and a wide range of intercalation levels in the $0 \leq x \leq 2$ range. The energy-dependent absorption coefficient $a(E)$ was then calculated between 0.5 and 4 eV.

Data on $a(E)$ were recorded for WO_{2.63}, WO_{2.89}, and WO_{2.93} films with various intercalation levels [78]. The absorption was found to rise steeply at $E > 3.5$ eV as a consequence of interband transitions across the fundamental band gap of W oxide and contributions from the ITO coating and the glass substrate. In order to clearly show the sub-band gap absorption in W oxide, the absorption coefficient for the non-intercalated film was subtracted from that of the intercalated ones. The ensuing result is shown in Fig. 2, where the reduced absorbance is denoted a^+ . The absorption coefficient has a maximum at ~ 1.5 eV, and it displays an initial increase as the intercalation level increases. Then the peak reaches saturation and finally decreases. The decrease takes place at the same time as another peak appears at higher energy. This

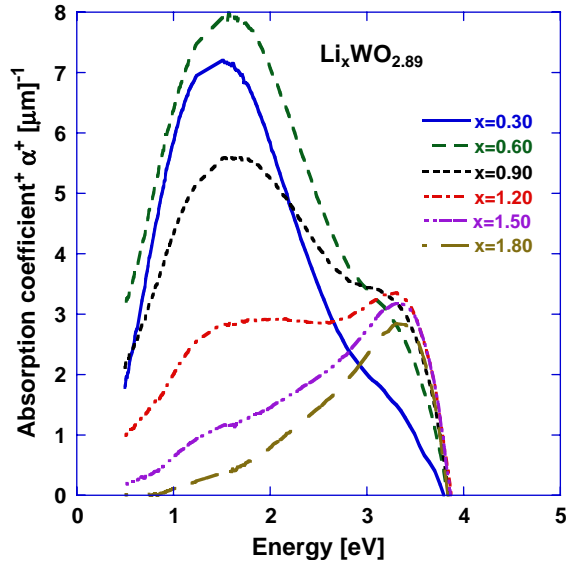


Fig. 2. Optical absorption coefficient a^+ vs. energy for a sub-stoichiometric amorphous $WO_{2.89}$ film intercalated to the shown Li/W ratios x . The absorption a for the unintercalated film has been subtracted.

behaviour continues until the new peak at ~ 3.3 eV takes over most of the absorption. The new peak is responsible for the brown colour observed when the intercalation level corresponds to $x > 0.7$.

Attempts to fit the spectra in Fig. 2 with two Gaussian peaks did not lead to satisfactory results, but a superposition of three Gaussian peaks provides good fits for all intercalation levels. Two of the peaks were fixed at the positions observed in the figure, viz. 1.4 eV (peak 1) and 3.37 eV (peak 3), while the position of the third feature (peak 2) was found to vary between 2.45 and 2.70 eV. Fig. 3 yields the integrated

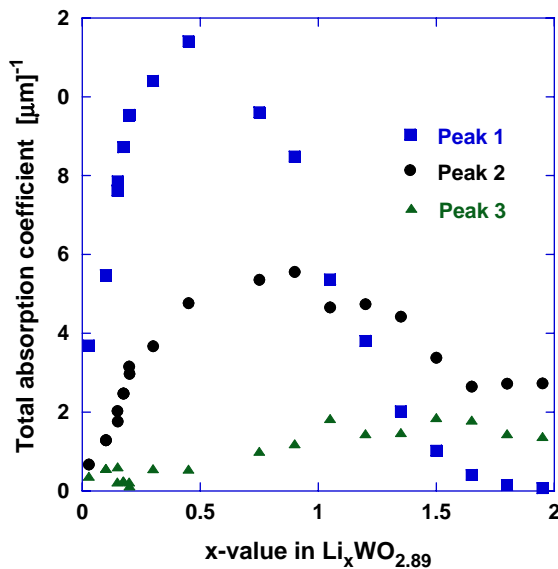


Fig. 3. Total absorption coefficient a vs. Li/W ratio x of three superimposed Gaussian peaks at energies being 1.4 eV (peak 1), 3.37 eV (peak 3), and 2.45–2.70 eV (peak 2). These peaks emerged from a fit to the absorption coefficients shown in Fig. 2, as discussed in the main text.

strengths of these Gaussian peaks as a function of x for the three films. It is seen that peak 1 is the highest; its maximum lies at $x \approx 0.5$ for all films. The peak increases as the oxygen deficiency increases. Peak 3, which has been fixed at 3.37 eV, increases continuously as the intercalation level increases and was highest for the film comprised of $WO_{2.63}$. Peak 2, whose position was allowed to vary during the fitting, is pronounced and it seems to be at a maximum for $0.5 < x < 1$. It should be pointed out that it was sometimes difficult to separate peaks 2 and 3.

What is the cause of these three absorption peaks? The site saturation model can be extended to take into account transitions between three kinds of sites, namely, those corresponding to W^{4+} , W^{5+} , and W^{6+} [78]. Each site is taken to be “empty” or “filled” not only with one “electron” but also with two. Starting with empty states (zero intercalation), most of the states will be singly occupied in the beginning. “Electron transitions” between “empty” and singly occupied states then are most common. As more single states are “filled,” there will be an increased probability that also doubly occupied states will be formed. Analytical expressions for the probabilities of the possible electronic transitions can be found [78] and are given by

$$W^{6+} \leftrightarrow W^{5+} : P = 2x(2 - x)^3 \tag{2a}$$

$$W^{5+} \leftrightarrow W^{4+} : P = 2x^3(2 - x) \tag{2b}$$

$$W^{6+} \leftrightarrow W^{4+} : P = x^2(2 - x)^2 \tag{2c}$$

These functions are depicted in Fig. 4. It is seen that the qualitative behaviour displays significant similarities with the experimental results in Fig. 3, thus lending credence to site saturation as the underlying cause. It has to be kept in mind that the absorption strength per transition may be different for the three cases, which conceivably accounts for the different heights of the peaks.

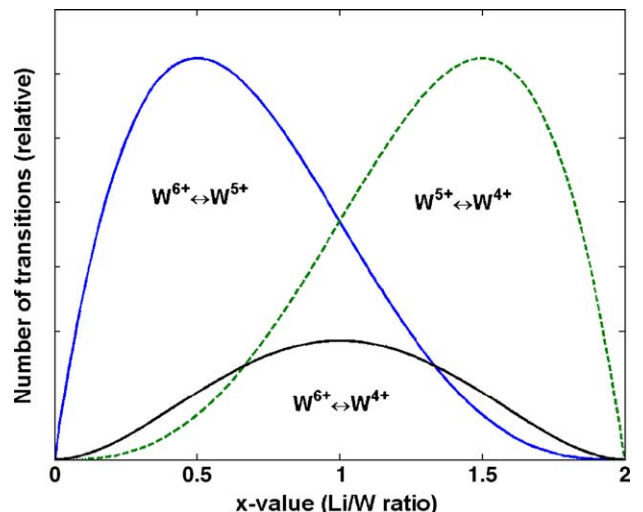


Fig. 4. Relative number for the transitions $W^{6+} \leftrightarrow W^{5+}$, $W^{5+} \leftrightarrow W^{4+}$, and $W^{6+} \leftrightarrow W^{4+}$ vs. Li/W ratio x , as given by the analytic expressions in Eqs. (2a,b,c).

4. On the electrochromism in Ni oxide films

4.1. Experimental

Ni oxide shows anodic electrochromism, as pointed out above. An extensive study of thin films of this material was performed recently [84]. Reactive DC magnetron sputtering was employed, using targets of magnetic Ni and non-magnetic $\text{NiV}_{0.08}$, in a plasma of $\text{Ar} + \text{O}_2 + \text{H}_2$ onto substrates of glass pre-coated with ITO (for optical and electrochemical measurements) and graphite (for compositional determinations using Rutherford Backscattering Spectrometry, RBS). The film thickness was ~ 200 nm. A range of other Ni-oxide-based films were investigated as well [60,85].

Three distinct deposition regions—here denoted 1, 2, and 3—can be identified when sputter deposition of nickel-oxide-based films is carried out under reactive conditions in a plasma of Ar with varying amounts of O_2 [85,86]. When this content is increased, the films evolve from nearly metallic (region 1) to transparent (region 2), and then from transparent to brown (region 3). Films in region 1 do not exhibit electrochromism, films belonging to region 2 have a very high activity and good charge capacity, and films in region 3 have low activity and poor optical properties. The deposition rate drops precipitously at the transition between regions 2 and 3; it was found to lie between 50 nm/min for a partly oxidized target and 10 nm/min in the over-oxidized mode of the target.

Elemental compositions were determined by RBS. Defining the composition as $\text{Ni}_{1-y}\text{V}_y\text{O}_z$, the three regions referred to above correspond to $y \approx 0.11$ and $z \leq 0.71$ for region 1, $0.05 \leq y \leq 0.10$ and $1.45 \leq z \leq 1.75$ for region 2, and $y \approx 0.11$ and $z \approx 2.07$ for region 3. These results are consistent with those of an independent ion beam analysis [87]. An increase of the O_2 flow in the gas mixture increased the oxygen content in the films. Furthermore, an addition of H_2 to the gas mixture produced films with improved crystallinity and also increased their charge capacity and transparency.

The density lies between 3.6 and 4.2 g/cm^3 in the optimized electrochromic films, obtained with intermediate O_2 and H_2 flows during the sputtering. At the transition between regions 1 and 2, the density was approximately 6.6 g/cm^3 , and at the transition to the over-oxidized region 3, it was approximately 4.9 g/cm^3 . Similar values of the density were found for nickel oxide films made by electron beam evaporation [24,88,89].

X-ray diffraction was used to study the structure of the as-deposited films. Specifically, bleached and colored films, made so that they belonged to region 2, exhibited cubic nickel oxide (Bunsenite) patterns, which is in agreement with previous work on NiO [24,90–96]. No evidence of phases containing hydrogen was found in any of the films. This, at first sight surprising, result can be understood if only the outermost part of the grains—that were too thin to be detectable [84]—take part in the electrochromic coloration.

Effective grain size and strain function were determined from the X-ray data. The effective grain size lay between 10 and 25 nm depending on the H_2 content during the thin film deposition. Small grain size, implying a large surface-to-bulk

ratio, may be beneficial for the electrochromic activity, as pointed out before [86,91,97]. Earlier work of ours [98] used extended X-ray absorption fine structure spectroscopy on films similar to the present ones and demonstrated that the vanadium atoms substitute nickel in a NiO-type structure, i.e., Ni and V appeared to form a mixed-oxide phase in the film.

Coloration and bleaching were conducted in an electrolyte of 1 M KOH with the film as working electrode in a three-electrode electrochemical cell.

4.2. Optical data: Coloration efficiency

Transmittance and reflectance were recorded by spectrophotometry in the as-deposited, colored, and bleached states. The main differences between these states are most prominent in the spectral transmittance within the visible region. Combining optical and electrochemical measurements, the spectral coloration efficiency (CE) was obtained from a standard relation [99].

Fig. 5 shows spectral CEs. The main effect of the electrochromism takes place in the ultraviolet and visible, whereas the coloration is small in the near-infrared. Three main peaks can be distinguished in Fig. 5: two prominent ones are located at wavelengths being 340 and 445 nm, and a third very broad peak can be discerned around 600 nm. This last peak was confirmed in other recordings of the CE. It is interesting to observe that the coloration efficiency is very high compared to values reported in other work [24,89,93,100], which is an important result with regard to applications. The influence of the sputtering conditions on the CE is strong at short wavelengths and weak at long wavelengths. The CEs correlate with the crystallinity of the films. The behavior supports the notion that the large inner surface area of the films is connected

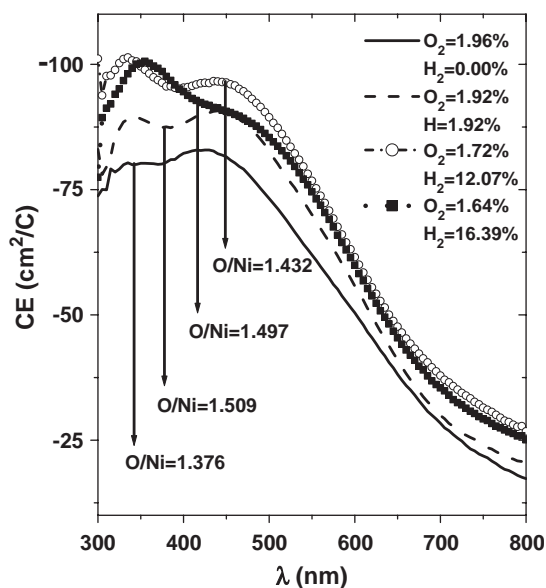


Fig. 5. Coloration efficiency (CE) vs. wavelength λ for $\text{Ni}_{1-y}\text{V}_y\text{O}_z$ films prepared with the shown fractions of O_2 and H_2 in the sputter plasma. Also shown are O/Ni ratios determined by RBS.

to the electrochromic activity, and that the coloration process takes place in the outermost parts of the grains.

Extensive work was carried out to ascertain the coloration mechanism. This work embraced X-ray photoemission spectroscopy using synchrotron radiation [101], several electrochemical analysis techniques including galvanometric intermittent titration [102], and infrared spectroscopy [102]. The results served as a confirmation of the basic correctness of the Bode reaction scheme [103,104].

5. Conclusion

This paper has given a brief review of the most recent work on inorganic electrochromic materials and devices. The emphasis on thin films of W oxide and Ni oxide was apparent. Furthermore, new results were presented on the optical properties of sputter deposited thin films of these two materials. For Li^+ intercalated sub-stoichiometric W oxide, it was shown that the absorption could be reconciled with an extended “site saturation” model accounting for electronic transitions between W ions in $6+$, $5+$, and $4+$ states. For H^+ de-intercalated Ni oxide, it was found that the coloration efficiency was higher than in prior studies, which presumably is a consequence of the nanocrystalline structure ensuing from the deposition conditions. The new findings on the optical absorption are of importance for developing more efficient and cost-effective devices for integration in “smart windows” capable of yielding energy efficiency and indoor comfort as well as for numerous other applications.

Acknowledgment

One of the authors (EA) thanks the University of Costa Rica for a scholarship for completing his PhD program at Uppsala University.

References

- [1] C.M. Lampert, C.G. Granqvist (Eds.), *Large-Area Chromogenics: Materials and Devices for Transmittance Control*, vol. IS4, SPIE Opt. Engr. Press, Bellingham, USA, 1990.
- [2] S.K. Deb, *Appl. Opt.*, Suppl. 3 (1969) 192.
- [3] S.K. Deb, *Philos. Mag.* 27 (1973) 801.
- [4] J.S.E.M. Svensson, C.G. Granqvist, *Sol. Energy Mater.* 11 (1984) 29.
- [5] J.S.E.M. Svensson, C.G. Granqvist, *Sol. Energy Mater.* 12 (1985) 391.
- [6] C.G. Granqvist, *Adv. Mater.* 15 (2003) 1789.
- [7] C.G. Granqvist, In: *Encyclopedia of Energy*, editor-in-chief C.J. Cleveland, Elsevier, Oxford, UK, (2004), Vol. 3, p. 845.
- [8] C.G. Granqvist, *Smart Mater. Bull.* (2002 (October)) 9.
- [9] A. Azens, C.G. Granqvist, *J. Solid State Electrochem.* 7 (2003) 64.
- [10] C.M. Lampert, *Sol. Energy Mater. Sol. Cells* 76 (2003) 489.
- [11] C.M. Lampert, *Mater. Today* (2004 (March)) 28.
- [12] H.J. Byker, *Electrochim. Acta* 46 (2001) 2015.
- [13] A.A. Argun, P.-H. Aubert, B.C. Thompson, I. Schwendeman, C.L. Gaupp, J. Hwang, N.J. Pinto, D.B. Tanner, A.G. MacDiarmid, J.R. Reynolds, *Chem. Mater.* 16 (2004) 4401.
- [14] I. Hamberg, C.G. Granqvist, *J. Appl. Phys.* 60 (1986) R123.
- [15] C.G. Granqvist, A. Hultåker, *Thin Solid Films* 411 (2002) 1.
- [16] D.S. Ginley, C. Bright, *MRS Bull.* 25 (8) (2000) 15.
- [17] P.P. Edwards, A. Porsch, M.O. Jones, D.V. Morgan, R.M. Perks, *Dalton Trans.* 19 (2004) 2995.
- [18] G. Leftheriotis, S. Papaefthimiou, P. Yanoulis, *Sol. Energy Mater. Sol. Cells* 61 (2000) 107.
- [19] S. Papaefthimiou, G. Leftheriotis, P. Yanoulis, *Electrochim. Acta* 46 (2001) 2145.
- [20] Z.-C. Wu, Z.-H. Chen, X. Du, J.M. Logan, J. Sippel, M. Nikolou, K. Kamaras, J.R. Reynolds, D.B. Tanner, A.F. Hebard, A.G. Rinzler, *Science* 305 (2004) 1273.
- [21] U. Schwarz-Schampera, P.M. Herzig, *Indium: Geology, Mineralogy, and Economics*, Springer, Berlin, 2002.
- [22] C. Marcel, J.-M. Tarascon, *Solid State Ionics* 143 (2001) 89.
- [23] K.-H. Heckner, A. Kraft, *Solid State Ionics* 152–153 (2002) 899.
- [24] C.G. Granqvist, *Handbook of Inorganic Electrochromic Materials*, Elsevier, Amsterdam, The Netherlands, 1995, (reprinted 2002).
- [25] P.M.S. Monk, R.J. Mortimer, D.R. Rosseinsky, *Electrochromism: Fundamentals and Applications*, VCH, Weinheim, Germany, 1995.
- [26] C.G. Granqvist, *Sol. Energy Mater. Sol. Cells* 60 (2000) 201.
- [27] C.G. Granqvist, E. Avendaño, A. Azens, *Thin Solid Films* 442 (2003) 201.
- [28] J. García-Cañadas, I. Mora-Seró, F. Fabregat-Santiago, J. Bisquert, G. García-Belmonte, *J. Electroanal. Chem.* 565 (2004) 329.
- [29] J. García-Cañadas, F. Fabregat-Santiago, I. Porqueras, C. Person, J. Bisquert, G. García-Belmonte, *Solid State Ionics* 175 (2004) 521.
- [30] A. Siokou, S. Ntais, S. Papaefthimiou, G. Leftheriotis, P. Yanoulis, *Surf. Sci.* 566–568 (2004) 1168.
- [31] R. Sivakumar, M. Jayachandran, C. Sanjeeviraja, *Mater. Chem. Phys.* 87 (2004) 439.
- [32] H.-N. Cui, S. Jia, L.-J. Meng, V. Teixeira, *Mikrochim. Acta* 145 (2004) 19.
- [33] H. Kamal, A.A. Akl, K. Abdel-Hady, *Physica B* 349 (2004) 192.
- [34] R. Sivakumar, A.M.E. Raj, B. Subramanian, M. Jayachandran, D.C. Trivendi, C. Sanjeeviraja, *Mater. Res. Bull.* 39 (2004) 1479.
- [35] A. Cremonesi, D. Bersani, P.P. Lottici, Y. Djaoued, P.V. Ashrit, *J. Non-Cryst. Solids* 345&346 (2004) 500.
- [36] G. Garcia-Belmonte, P.R. Bueno, F. Fabregat-Santiago, *J. Appl. Phys.* 96 (2004) 853.
- [37] G. Leftheriotis, S. Papaefthimiou, P. Yanoulis, *Sol. Energy Mater. Sol. Cells* 83 (2004) 115.
- [38] A. Patra, K. Auddy, D. Ganguli, J. Livage, P.K. Biswas, *Mater. Lett.* 58 (2004) 1059.
- [39] A. Pawlicka, D.C. Dragunski, K.V. Guimarães, C.O. Avellaneda, *Mol. Cryst. Liq. Cryst.* 416 (2004) 105.
- [40] R. Solarska, B.D. Alexander, J. Augustynski, *J. Solid State Electrochem.* 8 (2004) 748.
- [41] Yu.S. Krasnov, G.Ya. Kolbasov, *Electrochim. Acta* 49 (2004) 2425.
- [42] T. Pauporté, M.C. Bernard, Y. Soldo-Olivier, R. Faure, *J. Electrochem. Soc.* 151 (2004) H21.
- [43] T. Ivanova, K. Gesheva, F. Hamelmann, G. Popkirov, M. Abrashev, M. Ganchev, E. Tzvetkova, *Vacuum* 76 (2004) 195.
- [44] S.-H. Baeck, T.F. Jaramillo, D.H. Jeong, E.W. McFarland, *Chem. Commun.* (2004) 390.
- [45] K.R. Padmanabhan, *Nucl. Instrum. Methods Phys. Res., B Beam Interact. Mater. Atoms* 219–220 (2004) 942.
- [46] D. Yang, L. Xue, *Thin Solid Films* 469–470 (2004) 54.
- [47] N.R. de Tacconi, C.R. Chenthamrakshan, K.L. Wouters, F.M. MacDonnell, K. Rajeshwar, *J. Electroanal. Chem.* 566 (2004) 249.
- [48] M. Yuan, Y. Lu, B. Tian, H. Yang, B. Tu, J. Kong, D. Zhao, *Chem. Lett.* 10 (2004) 1396.
- [49] A. Medina, J.L. Solis, J. Rodriguez, W. Estrada, *Sol. Energy Mater. Sol. Cells* 80 (2004) 473.
- [50] Y. Jung, J. Lee, Y. Tak, *Electrochem. Solid-State Lett.* 7 (2004) H5.
- [51] J. Yano, K. Noguchi, S. Yamasaki, S. Yamasaki, *Electrochem. Commun.* 6 (2004) 110.
- [52] J. Backholm, A. Azens, G.A. Niklasson, *Sol. Energy Mater. Sol. Cells*, (in press).
- [53] L. Ottaviano, A. Pennisi, F. Simone, A.M. Salvi, *Opt. Mater.* 27 (2004) 307.
- [54] C.-G. Wu, M.-H. Chung, *J. Solid State Chem.* 177 (2004) 2285.

- [55] K.D. Lee, W.C. Jung, *J. Korean Phys. Soc.* 45 (2004) 447.
- [56] I. Bouessay, A. Rougier, J.-M. Tarascon, *J. Electrochem. Soc.* 151 (2004) H145.
- [57] R. Cerc Korošec, P. Bukovec, *Thermochim. Acta* 410 (2004) 65.
- [58] L. Ottaviano, A. Pennisi, F. Simone, *Surf. Interface Anal.* 36 (2004) 1335.
- [59] K. Nakaoka, J. Ueyama, K. Ogura, *J. Electroanal. Chem.* 571 (2004) 93.
- [60] E. Avendaño, A. Azens, G.A. Niklasson, C.G. Granqvist, *Sol. Energy Mater. Sol. Cells* 84 (2004) 337.
- [61] F.F. Ferreira, M.C.A. Fantini, *Solid State Ionics* 175 (2004) 517.
- [62] G. Eranna, B.C. Joshi, D.P. Runthala, R.P. Gupta, *Crit. Rev. Solid State Mater. Sci.* 29 (2004) 111.
- [63] S.-H. Lee, S.-K. Joo, *Sol. Energy Mater. Sol. Cells* 39 (1995) 155.
- [64] J.H.G. Mathew, S.P. Sapers, M.J. Cumbo, N.A. O'Brien, R.B. Sargent, V.P. Raksha, R.B. Ladaherne, B.P. Hichwa, *J. Non-Cryst. Solids* 218 (1997) 342.
- [65] A. Azens, L. Kullman, G. Vaivars, H. Nordborg, C.G. Granqvist, *Solid State Ionics* 113–115 (1998) 449.
- [66] R. Lechner, L.K. Thomas, *Sol. Energy Mater. Sol. Cells* 54 (1998) 139.
- [67] J. Nagai, G.D. McMeeking, Y. Saitoh, *Sol. Energy Mater. Sol. Cells* 56 (1999) 309.
- [68] J. Karlsson, A. Roos, *Solar Energy* 68 (2000) 493.
- [69] A. Azens, G. Vaivars, M. Veszelei, L. Kullman, C.G. Granqvist, *J. Appl. Phys.* 89 (2001) 7885.
- [70] K.-S. Ahn, Y.-C. Nah, Y.-E. Sung, K.-Y. Cho, S.-S. Shin, J.-K. Park, *Appl. Phys. Lett.* 81 (2002) 3930.
- [71] K.-S. Ahn, Y.-C. Nah, J.-Y. Park, Y.-E. Sung, K.-Y. Cho, S.-S. Shin, J.-K. Park, *Appl. Phys. Lett.* 82 (2003) 3379.
- [72] C. Person, I. Porqueras, M. Vives, C. Corbella, A. Pinyol, E. Bertran, *Solid State Ionics* 165 (2003) 73.
- [73] A.-K. Jonsson, M. Furlani, G.A. Niklasson, *Sol. Energy Mater. Sol. Cells* 84 (2004) 361.
- [74] A.-L. Larsson, G.A. Niklasson, *Sol. Energy Mater. Sol. Cells* 84 (2004) 351.
- [75] A.-L. Larsson, G.A. Niklasson, *Mater. Lett.* 58 (2004) 2517.
- [76] A. Azens, G. Gustavsson, R. Karmhag, C.G. Granqvist, *Solid State Ionics* 165 (2003) 1.
- [77] A. Azens, E. Avendaño, C.G. Granqvist, *Proc. Soc. Photo-Opt. Instrum. Eng.* 5123 (2003) 185.
- [78] L. Berggren, *Optical Absorption and Electrical Conductivity in Lithium Intercalated Amorphous Tungsten Oxide Films*, PhD thesis, Uppsala University, Sweden, 2004 (unpublished).
- [79] M. Stolze, B. Camin, F. Galbert, U. Reinholz, L.K. Thomas, *Thin Solid Films* 409 (2002) 254.
- [80] C. Bechinger, M.S. Burdis, J.-G. Zhang, *Solid State Commun.* 101 (1997) 753.
- [81] S.-H. Lee, H.M. Cheong, C.E. Tracy, A. Mascharenhas, A.W. Czanderna, S.K. Deb, *Appl. Phys. Lett.* 75 (1999) 1541.
- [82] T.J. Vink, E.P. Boonekamp, R.G.F.A. Verbeek, Y. Tamminga, *J. Appl. Phys.* 85 (1999) 1540.
- [83] M. Denesuk, D.R. Uhlmann, *J. Electrochem. Soc.* 143 (1996) L186.
- [84] E. Avendaño, *Electrochromism in Nickel-Based Oxides: Coloration Mechanisms and Optimization of Sputter-Deposited Thin Films*, PhD thesis, Uppsala University, 2004 (unpublished).
- [85] E. Avendaño, A. Azens, J. Isidorsson, R. Karmhag, G.A. Niklasson, C.G. Granqvist, *Solid State Ionics* 165 (2003) 169.
- [86] E. Avendaño, A. Azens, G. Niklasson, *Proc. Soc. Photo-Opt. Instrum. Eng.* 4458 (2001) 154.
- [87] W. Wagner, F. Rauch, K. Bange, *Nucl. Instrum. Methods Phys. Res., B Beam Interact. Mater. Atoms* 89 (1994) 104.
- [88] A. Agrawal, H.R. Habibi, R.K. Agrawal, J.P. Cronin, D.M. Roberts, R. Caron-Popowich, C.M. Lampert, *Thin Solid Films* 221 (1992) 239.
- [89] K. Bange, in: H. Bach, D. Krause (Eds.), *Thin Films on Glass*, Springer, Berlin, 1997, (Chapter 4).
- [90] J. Scarminio, W. Estrada, A. Andersson, A. Gorenstein, F. Decker, *J. Electrochem. Soc.* 139 (1992) 1236.
- [91] E.L. Miller, K.E. Rocheleau, *J. Electrochem. Soc.* 144 (1997) 1995.
- [92] W. Estrada, A.M. Andersson, C.G. Granqvist, *J. Appl. Phys.* 64 (1988) 3678.
- [93] D.A. Wruck, M.A. Dixon, M. Rubin, N. Bogy, *J. Vac. Sci. Technol., A* 9 (2001) 2170.
- [94] K. Yoshimura, T. Miki, S. Tanemura, *Jpn. J. Appl. Phys.* 34 (1995) 2440.
- [95] K. Yoshimura, T. Miki, S. Tanemura, *Mater. Res. Bull.* 32 (1997) 839.
- [96] I.C. Faria, M. Kleinke, A. Gorenstein, M.C.A. Fantini, M.H. Tabacniks, *J. Electrochem. Soc.* 145 (1998) 235.
- [97] A. Azens, L. Kullman, G. Vaivars, H. Nordborg, C.G. Granqvist, *Solid State Ionics* 113–115 (1998) 449.
- [98] E. Avendaño, A. Kuzmin, J. Purans, A. Azens, G.A. Niklasson, C.G. Granqvist, *Phys. Scr. T* 115 (2005) 464.
- [99] A. Azens, A. Talledo, A.M. Andersson, G.A. Niklasson, B. Stjerna, C.G. Granqvist, *Proc. Soc. Photo-Opt. Instrum. Eng.* 1728 (1992) 103.
- [100] M. Kitao, K. Izawa, S. Yamada, *Sol. Energy Mater. Sol. Cells* 39 (1995) 115.
- [101] E. Avendaño, A. Azens, G.A. Niklasson, C.G. Granqvist, (in press).
- [102] E. Avendaño, A. Azens, G.A. Niklasson, C.G. Granqvist, *J. Electrochem. Soc.*, (in press).
- [103] H. Bode, K. Dehmelt, J. Witte, *Electrochim. Acta* 11 (1966) 1079.
- [104] H. Bode, K. Dehmelt, J. Witte, *Z. Anorg. Allg. Chem.* 366 (1969) 1.